Dalton Transactions

Accepted Manuscript

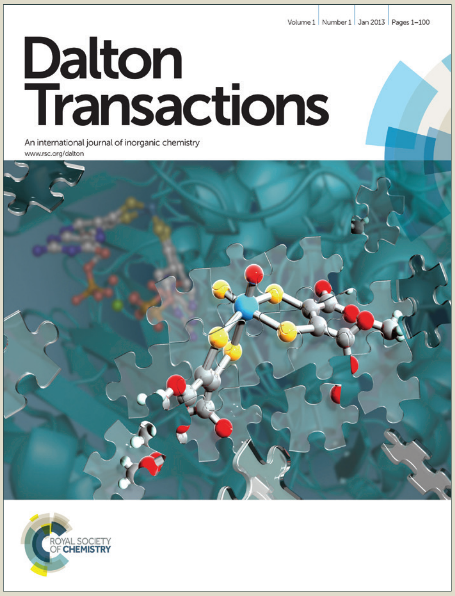

ROYAL SOCIETY OF CHEMISTRY

www.rsc.org/dalton

Journal Name RSCPublishing

ARTICLE

Deformation twinning of ferrocene crystals assisted by the rotational mobility of cyclopentadienyl rings

Cite this: DOI: 10.1039/x0xx00000x

Yasuhiro Miyamoto[a] and Satoshi Takamizawa*[a]

Received 00th January 2012,
Accepted 00th January 2012

DOI: 10.1039/x0xx00000x

www.rsc.org/

Deformation twinning, which is a type of plastic deformation, has been especially investigated in metal materials. However, only a few examples are found in organic solids. We observed mechanical twinning deformation on a simple ferrocene crystal, which is considered the most representative organometallic compound, and evaluated the crystal structures under the twinning state and the shear deformation characteristics by single-crystal X-ray diffraction analysis and uniaxial compression tests. The structural analyses showed the molecular rearrangement during twinning deformation. The shear deformation properties depend on the rotational mobility of the cyclopentadienyl rings in comparison with crystals of nickelocene, ruthenocene, and mixed crystals of ferrocene/ruthenocene.

Introduction

In general, solids deform elastically after sufficient stress is applied and then eventually deform plastically. Plastic deformation is accompanied by slip or twinning deformation. There are only a few reports on classical compression or shearing test on organic crystals. The bulk measurements can provide the practical mechanical properties of solids with the integration of micro- and macro-scale phenomena including bulk transition although the modern procedures such as nanoindentation,[1] which can detect the local elasticity and plasticity in microscale, are known as all-around methods for materials.

Twinning deformation in organic solids has been reported for $(TMTSF)_2X$[2] (X = ClO_4, PF_6, AsF_6, and NO_3), 1,3,5-tribromo-2,4,6-triiodobenzene[3], 1,3,5-trichloro-2,4,6-triiodobenzene[3], L-lysine monohydrochloride hydrate[4], and adipic acid doped with 3-methyl adipic acid[5]. All these compounds have planar molecular structures.

Ferrocene, which is one of the most important discoveries in the history of organometallics, has a sandwich structure that has the Fe(II) ion caught between two cyclopentadienyl rings, and its molecular shape can be considered to be nearly spherical. The crystal structures[6-8], thermally induced structural phase transitions[9-11], and molecular mobilities[12,13] of ferrocene have been studied, but the mechanical properties have not been of much interest up to now.

We observed twinning deformation in a single crystal of ferrocene by applying shear stress and found a correlation between twinning deformation and the rotational mobility of the cyclopentadienyl rings by using single-crystal X-ray diffraction analysis and uniaxial compression tests.

Results and discussion

Single crystals of ferrocene that were rhombic and 300-500 μm long were obtained by vacuum sublimation. Single-crystal X-ray diffraction analysis at 298K indicated that the crystal structure was monoclinic $P2_1/n$ （a = 5.9252 Å, b = 7.6035 Å, c = 9.0354 Å, β = 93.165°）, which corresponded with a previous report[5]. By applying shear stress to the crystal, twinning deformation occurred. After unloading, the deformed shape did not recover, leaving a residual strain.

Figure 1 (a) shows the face correlations of the twinning interfaces determined by X-ray analysis on the mechanically twined crystals. We named the mother phase "α_0" and the daughter phase as "α_1", which was generated with the twinning deformation. The twinning interface was $(011)\alpha_0//(0\bar{1}\bar{1})\alpha_1$, $(011)\alpha_0//(0\bar{1}1)\alpha_1$, $(01\bar{1})\alpha_0//(011)\alpha_1$, or $(01\bar{1})\alpha_0//(0\bar{1}1)\alpha_1$, which are equivalent to each other. We discuss the twinning crystal in the case of $(011)\alpha_0//(0\bar{1}\bar{1})\alpha_1$ because the deformed shapes and the crystal structures under the twinning state are isomorphic in all the twinning interfaces. The surface indexes of α_0 and α_1 in each interface are summarized in Table 1 based on the deformed shape.

Table 1. Summary of equivalent face indexes of crystals α_0 and α_1.

α_0			α_1		
Inter face	Front surface	Upper surface	Inter face	Front surface	Upper surface
(011)	$(01\bar{1})$	$(10\bar{1})$	$(0\bar{1}\bar{1})$	$(0\bar{1}1)$	$(\bar{1}\bar{1}0)$
(011)	$(01\bar{1})$	$(10\bar{1})$	$(0\bar{1}1)$	$(0\bar{1}\bar{1})$	$(1\bar{1}0)$
$(01\bar{1})$	(011)	$(\bar{1}01)$	$(0\bar{1}\bar{1})$	$(0\bar{1}1)$	$(\bar{1}\bar{1}0)$
$(01\bar{1})$	(011)	$(\bar{1}01)$	$(0\bar{1}1)$	$(0\bar{1}\bar{1})$	$(1\bar{1}0)$

(See the underlined face correlation in Fig. 1.)

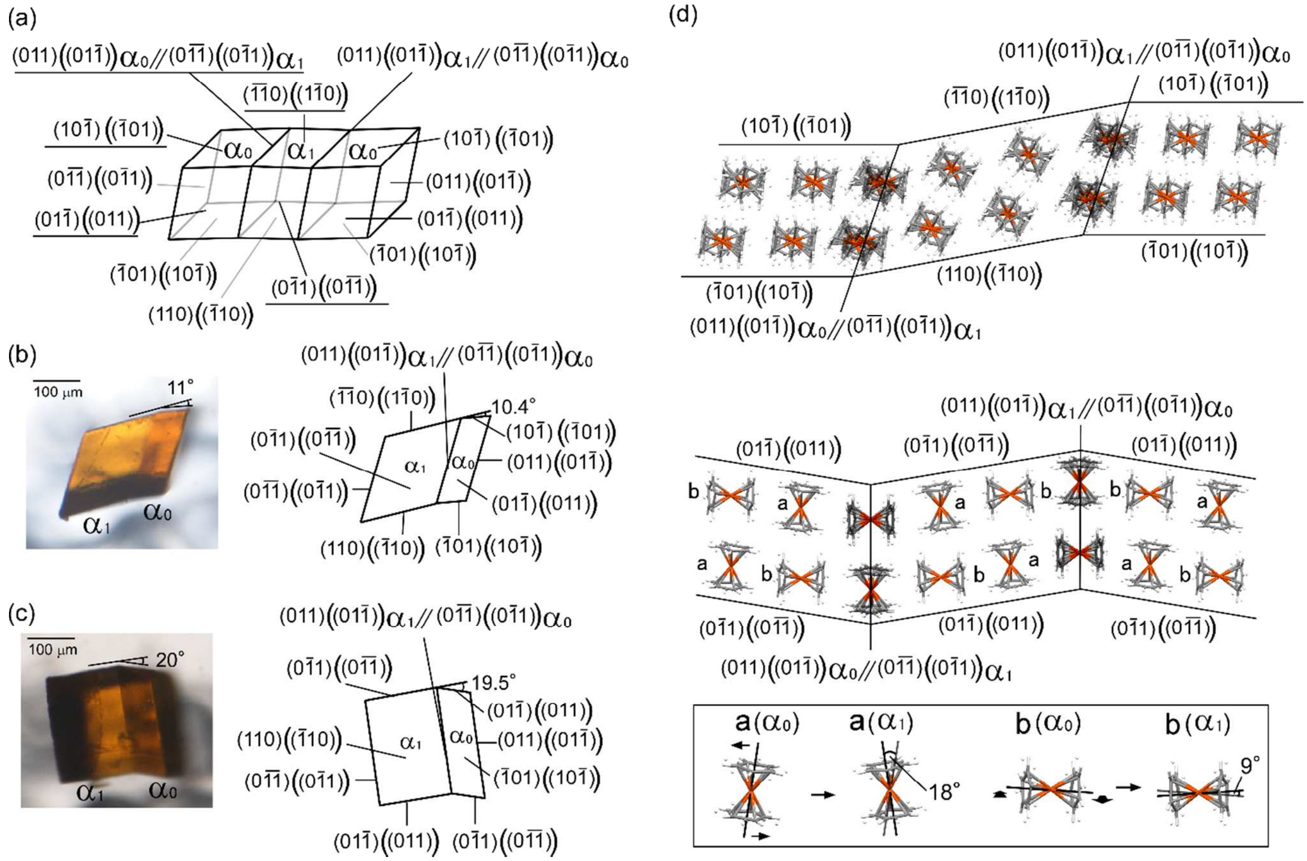

Fig. 1. (a) Surface indexes of mechanically twinned crystal. (b), (c) Photographs of mechanically twinned crystal that were projected to $[1\bar{1}1]\alpha_0$ ($[\bar{1}\bar{1}\bar{1}]\alpha_0$) (b) and $[\bar{1}00]\alpha_0$ ($[100]\alpha_0$) (c), and their pattern diagrams. (d) Crystal structures under twinning state which were projected to $[1\bar{1}1]\alpha_0$ ($[\bar{1}\bar{1}\bar{1}]\alpha_0$) (upper figure) and $[\bar{1}00]\alpha_0$ ($[100]\alpha_0$) (lower figure), and molecular arrangement in α_0 and α_1.

The bending angles were observed with a microscope to be 11° and 20°, judging from the projection direction of $[1\bar{1}1]\alpha_0$ and $[\bar{1}00]$ (Fig. 1 (b), (c)), respectively, which agreed with the expected angles from X-ray data of 10.4° and 19.5°. This agreement clearly demonstrates that the macroscopic structural change corresponded with the microscopic structural change.

Figure 1 (d) shows the crystal structures under the twinning state projected to $[1\bar{1}1]\alpha_0$ and $[\bar{1}00]\alpha_0$. Every twinning interface is a mirror plane. Therefore, considering only the lattice, strain cannot occur at the interface. However, strain can occur on the molecules at the twinning boundary since the molecular arrangement changes at the boundary. Molecules **a** and **b**, whose molecular axes are skewed from each other, are each distinguished on the basis of molecular orientation. Projected on $[\bar{1}00]\alpha_0$, the molecular axes of **a**(α_1) and **b** (α_1) slants by 18° and 9° to that of **a**(α_0) and **b** (α_0), respectively, which requires molecular rearrangement during twinning deformation.

It has been known that the cyclopentadienyl rings rotate on molecular axes in crystalline ferrocene, and there is a possibility that this rotation correlates with twinning deformation. Therefore, we checked the crystal deformation properties for nickelocene and ruthenocene under shear stress to investigate the effect of the rotational mobility of cyclopentadienyl rings on twinning deformation. The crystal structure of nickelocene (Monoclinic *P2₁/n*) is isomorphous to the high-temperature phase of ferrocene[14] and that of ruthenocene (Orthorhombic *Pnma*) is isomorphous to the low-temperature phase of ferrocene[15]. The average residence times of cyclopentadienyl rings in each of the five possible orientations at 303 K are 3.9×10^{-12} s in nickelocene[12] and 4.1×10^{-10} s in ruthenocene[13]. As compared to 4.3×10^{-12}s in ferrocene[12], nickelocene has almost the same value but ruthenocene has about a hundredth of that. Thus, only ruthenocene shows low rotational mobility. As shown in Fig. 2(a), crystals of nickelocene showed isomorphic twinning deformation with ferrocene by applying shear stress. However, we could not observe twinning deformation in the ruthenocene crystals and could only observe fractures (Fig. 2(b)).

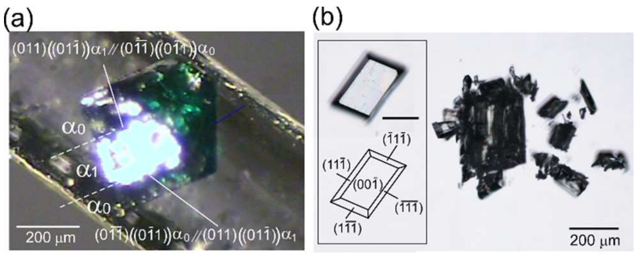

Fig. 2. Photographs of a mechanically twined nickelocene crystal (a) and a fractured ruthenocene crystal (b).

In comparing elasticity and plasticity between the ferrocene and ruthenocene crystals, we performed uniaxial compression tests under a microscope. We found that ferrocene crystals showed lower elastic modulus and more plastic nature than those of ruthenocene crystals. Figure 3 shows stress-strain curves measured along the normal directions of $FeCp_2$ (10$\bar{1}$), $FeCp_2$ (011) ((01$\bar{1}$)), and $RuCp_2$ (001). The S-S curves of ferrocene and ruthenocene indicated ductility and brittleness, respectively. By pushing the (10$\bar{1}$) surface, first, the ferrocene crystal showed elastic deformation. As the stress and strain reached 5.7 MPa and 0.0187, twinning deformation occurred and the entire crystal phase changed from α_0 to α_1. As a result of the decrease in thickness during the twinning deformation, the strain increased to 0.0985 and the stress decreased to 2.61 MPa. After further compression was applied, the crystal yielded mainly by the slippage with a stress of 4-8 MPa and a strain of 0.103-0.145. Compressed in the normal direction of (011) ((01$\bar{1}$)), which intersects with that of (10$\bar{1}$) at 70.6°, the crystal yielded with a stress of 1.5-3.6 MPa and a strain of 0.03-0.06. This means that yield stress depends on crystal orientation. In contrast, the ruthenocene showed only elastic deformation. The crystal fractured at a stress of 97.96 MPa and strain of 0.059. We estimated Young's moduli as 1.1 GPa ($FeCp_2$ (10$\bar{1}$)), 0.3 GPa ($FeCp_2$ (011)), and 6.4 GPa ($RuCp_2$ (001)) based on each elastic deformation area, clearly showing that Young's modulus of ferrocene is five times smaller than that of ruthenocene.

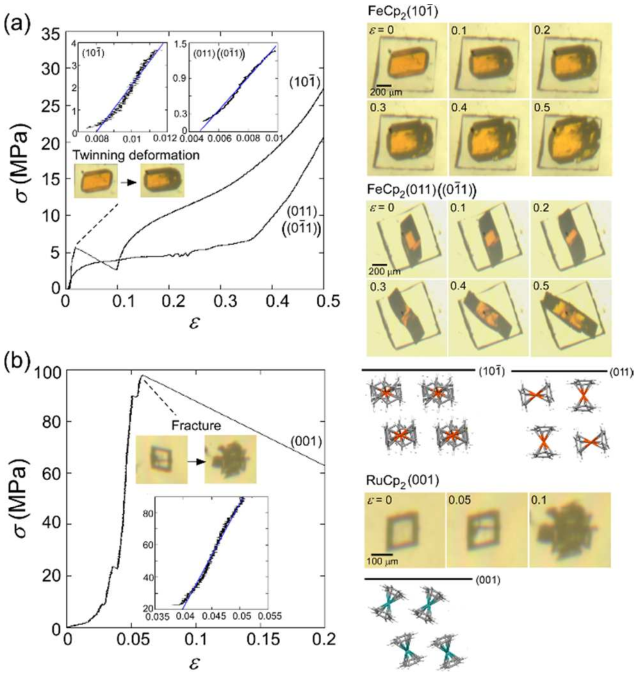

Fig. 3. Stress-strain curves at 20°C. (a) Normal direction of $FeCp_2$ (10$\bar{1}$) (compression area: 142,955 μm^2, thickness: 169 μm, compression speed: 84.5 μm min^{-1}) and that of $FeCp_2$ (011) ((01$\bar{1}$)) (compression area: 92,912 μm^2, thickness: 445 μm, compression speed: 44.5 μm min^{-1}). (b) Normal direction of $RuCp_2$ (001) (compression area: 10,096 μm^2, thickness: 75 μm, compression speed: 37.4 μm min^{-1}). The values of Young's modulus were 1.1 GPa ($FeCp_2$ (10$\bar{1}$)), 0.3 GPa ($FeCp_2$ (011)), and 6.4 GPa ($RuCp_2$ (001)), which were estimated from the inset graphs by using the least-square method (blue line). Photographs were taken along the direction of the compression. The crystal packing views are drawn in the perpendicular direction of compression.

It is thought that the twinning deformation strongly correlates to the rotational mobility of the cyclopentadienyl rings or the difference in crystal lattice since mechanical twinning occurred easily in ferrocene and nickelocene but was not observed in ruthenocene. To confirm this possibility, we prepared 11.0% ruthenocene-doped crystals ($\{(FeCp_2)_{0.89}(RuCp_2)_{0.11}\}$), which were isomorphous to the high-temperature phase of ferrocene. In applying shear force to this mixed crystal, we could not find twinning deformation (Fig. S6), which indicates a correlation between the rotation mobility of the cyclopentadienyl rings and twinning deformation. It appears that ruthenocene, which had remarkably low rotational mobility of its cyclopentadienyl rings, caused the molecular rearrangement barrier during the twinning deformation and hampered mechanical twinning in the mixed crystals.

Experimental

Preparation of crystals

Reagent-grade ferrocene, nickelocene, and ruthenocene were purchased from Tokyo Chemical Industry Co., Ltd. Yellow rhombic single crystals of ferrocene with a size of 300-500 μm and green polygonal single crystals of nickelocene with a size of 300-500 μm were prepared by vacuum sublimation at 1 kPa, 60 °C. Pale-yellow rhombic single crystals of ruthenocene with a size of 150-300 μm were prepared by evaporation of its toluene solution. Yellow rhombic crystals of ruthenocene-doped ferrocene ($\{(FeCp_2)_{0.89}(RuCp_2)_{0.11}\}$) with a size of 100-250 μm were prepared by evaporation of a toluene solution of the ferrocene /ruthenocene mixture (6:1 (mol/mol)).

UV-VIS spectrum measurement

The composition of the mixed crystals was determined from a UV-VIS spectrum recorded by a V-630, Nippon Bunko Co., Ltd. A 10.0-mM toluene solution of ferrocene and a 2.3-mM toluene solution of ruthenocene were used as standard solutions. The simulated absorption spectrum in which the molar ratio of ferrocene and ruthenocene was 8.0: 1.0 (9.6 mM: 1.2 mM) reproduced the spectrum of the toluene solution in which the ruthenocene-doped ferrocene crystals were dissolved. Thus, the composition of the mixed crystals was calculated to be $(FeCp_2)_{0.89}(RuCp_2)_{0.11}$. The UV-VIS spectra are summarized in Fig. S7.

Deformation and breakdown behavior of crystals

Twinning deformation of the ferrocene crystals was achieved by pushing a metal needle against the surface (10$\bar{1}$). The same pushing procedure was applied for the ferrocene and nickelocene crystals. For the preparation of twin crystals of nickelocene, the pushed crystal surface and generated interface were unspecified due to the difficulty in face indexing. The breakdown behavior of the ruthenocene and ruthenocene-doped ferrocene crystals was observed by pushing on the (001) and $(10\bar{1})$ surfaces, respectively.

Single-Crystal X-ray Diffraction Experiment

All single-crystal X-ray analyses were performed on a Bruker Smart APEX CCD area detector using graphite-monochromated Mo-Kα radiation (λ = 0.71073 Å). Data collections were performed at room temperature (292-300 K). Empirical absorption corrections were applied using SADABS software. The structures were solved by the direct method (SHELXS-97) and refined by full-matrix least squares calculations on F^2 (SHELXL-97) using the SHELX-TL program package. Non-hydrogen atoms were refined anisotropically; hydrogen atoms were fixed at calculated positions and refined using a riding model. Crystal phase indexing was performed using SMART in a SHELXTL Ver. 6.12 program package. The crystallographic data are summarized in Table. S1-S3. CCDC-1039774-1039780, 1046676 contains the supplementary crystallographic data for this paper.

Uniaxial Compression Tests

All uniaxial compression tests were performed at 20 °C on a universal testing machine (Tensilon RTG-1210, A&D Co., Ltd) under microscope observation. A compression test in the normal direction of $FeCp_2$ $(10\bar{1})$ (169 μm thick and 142955 μm^2 compression area) was performed at a compression speed of 84.5 $\mu m\ min^{-1}$ and that of ferrocene (011) ($(0\bar{1}1)$) (445 μm thick, 92912 μm^2 compression area) was performed at a compression speed of 44.5 $\mu m\ min^{-1}$. A compression test in the normal direction of ruthenocene (001) (75 μm thick, 10096 μm^2 compression area) was performed at a compression speed of 37.4 $\mu m\ min^{-1}$. We did not conduct a compression test of nickelocene because its air sensitivity and crystal shape made accurate measurement difficult.

Conclusions

A crystal of ferrocene, which is considered the most representative organometallic compound, shows twinning deformation through the application of shear force. Its twinning deformation stress is 3.7 MPa, Young's modulus is 1.1 GPa, and yield stress is in the range of 4-8 MPa according to the result of a $(10\bar{1})$ compression test. The twinning interfaces are $(011)\alpha_0//(0\bar{1}\bar{1})\alpha_1$, $(011)\alpha_0//(0\bar{1}1)\alpha_1$, $(01\bar{1})\alpha_0//(011)\alpha_1$, or$(01\bar{1})\alpha_0//(0\bar{1}1)\alpha_1$, which are basically equivalent mirror planes.

A crystal of nickelocene, which is isomorphous to the high-temperature phase of ferrocene and has cyclopentadienyl rings with rotational mobility similar to that of ferrocene, also shows twinning deformation, but a crystal of ruthenocene, which is isomorphous to the low-temperature phase of ferrocene and has markedly low rotational mobility, did not show twinning deformation. It appears that the rotational mobility of the cyclopentadienyl rings assists in the molecular rearrangement and twinning deformation in ferrocene and nickelocene.

Acknowledgements

This work was partially supported by a Research Grant, Izumi Science & Technology Foundation and SUZUKI Foundation for S.T.

Notes and references

[a] Department of Materials System Science; Graduate School of Nanobioscience; Yokohama City University; 22-2 Seto; Kanazawa-ku, Yokohama, Kanagawa 236-0027; Japan.
E-mail: staka@yokohama-cu.ac.jp

† Electronic Supplementary Information (ESI) available: [details of any supplementary information available should be included here]. See DOI: 10.1039/b000000x/

1 S. Varughese, M. S. R. N. Kiran, U. Ramamurty, G. R. Desiraju, *Angew. Chem. Int. Ed*., 2013, **52**, 2701
2 H. Schwenk, K. Neumair, K. Andres, F. Wudl, and E. Aharon-Shalom, *Mol. Cryst. Liq. Cryst*., 1982, **79**, 277.
3 C. M. Reddy, M. T. Kirchner, R. C. Gundakaram, K. A. Padmanabhan, and G. R. Desiraju, *Chem. —Eur. J.,* 2006, **12**, 2222.
4 R. Bandyopadhyay, D. J. W. Grant, *Pharm. Res.,* 2002, **19**, 491.
5 L. Williams-Seton, R. J. Davey, H. F. Lieberman, R. G. Pritchard, *J. Pharm. Sci*., 2000, **89**, 346.
6 P. Seiler, J. D. Dunitz, *Acta Crystallogr., Sect. B: Struct. Crystallogr. Cryst. Chem*., 1979, **35**, 1068.
7 P. Seiler, J. D. Dunitz, *Acta Crystallogr., Sect. B: Struct. Crystallogr. Cryst. Chem*., 1982, **38**, 1741.
8 P. Seiler, J. D. Dunitz, *Acta Crystallogr., Sect. B: Struct. Crystallogr. Cryst. Chem*., 1979, **35**, 2020.
9 J. W. Edwards, G. L. Kington, R. Mason, *Trans. Faraday. Soc*., 1960, **56**, 660.
10 J. W. Edwards, G. L. Kington, *Trans. Faraday. Soc*., 1962. **58**. 1334.
11 K. Ogasahara, M. Sorai, H. Suga, *Chem. Phys. Lett*., 1979, **68**, 457.
12 A. B. Gardner, J. Howard, T. C. Waddington, R. M. Richardson, J. Tomkinson, *Chem. Phys*., 1981, **57**, 453.
13 A. J. Campbell, C. A. Fyfe, D. Harold-Smith, K. R. Jeffrey, *Mol. Cryst. Liquid Cryst*., 1976, **36**, 1.
14 P. Seiler, J. D. Dunitz, *Acta Crystallogr., Sect. B: Struct. Crystallogr. Cryst. Chem*., 1980, **36**, 2255.
15 P. Seiler, J. D. Dunitz, *Acta Crystallogr., Sect. B: Struct. Crystallogr. Cryst. Chem*., 1980, **36**, 2946.

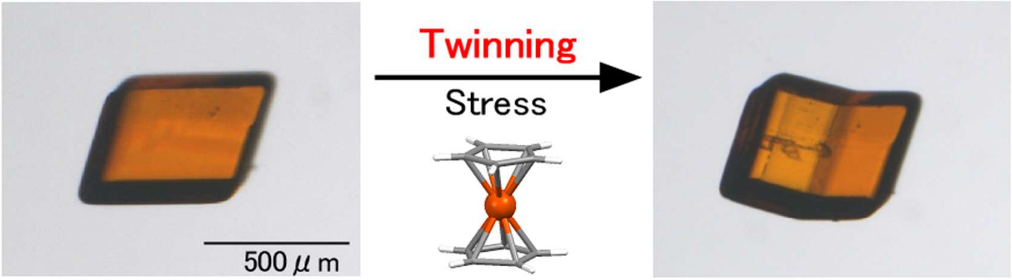

A mechanical load lets ferrocene crystals become a twinning through the rotational mobility of cyclopentadienyl rings.